



**HAL**  
open science

## Expected masses of merging compact object binaries observed in gravitational waves

Tomasz Bulik, Dorota Gondek-Rosinska, Krzysztof Belczynski

► **To cite this version:**

Tomasz Bulik, Dorota Gondek-Rosinska, Krzysztof Belczynski. Expected masses of merging compact object binaries observed in gravitational waves. *Monthly Notices of the Royal Astronomical Society*, 2004, 352, pp.1372-1380. 10.1111/j.1365-2966.2004.08028.x . hal-03801292

**HAL Id: hal-03801292**

**<https://hal.science/hal-03801292v1>**

Submitted on 23 Feb 2023

**HAL** is a multi-disciplinary open access archive for the deposit and dissemination of scientific research documents, whether they are published or not. The documents may come from teaching and research institutions in France or abroad, or from public or private research centers.

L'archive ouverte pluridisciplinaire **HAL**, est destinée au dépôt et à la diffusion de documents scientifiques de niveau recherche, publiés ou non, émanant des établissements d'enseignement et de recherche français ou étrangers, des laboratoires publics ou privés.

# Expected masses of merging compact object binaries observed in gravitational waves

T. Bulik,<sup>1\*</sup> D. Gondek-Rosinska<sup>1,2,3</sup> and K. Belczynski<sup>4</sup>

<sup>1</sup>*Nicolaus Copernicus Astronomical Centre, Bartycka 18, 00716 Warsaw, Poland*

<sup>2</sup>*LUTH, Observatoire de Paris, Place Jules Janssen, 92195 Meudon Cedex, France*

<sup>3</sup>*Universite Paris 7 Denis-Diderot, 2 place Jussieu 75251 Paris, France*

<sup>4</sup>*Northwestern University, 2145 Sheridan Road, Evanston, IL 60208, USA*

Accepted 2004 May 13. Received 2004 May 12; in original form 2003 October 7

## ABSTRACT

We use the well-tested STARTRACK binary population synthesis code to examine the properties of the population of compact object binaries. We calculate the distribution of masses and mass ratios, taking into account weights introduced by observability in gravitational waves during inspiral. We find that in the observability-weighted distribution of double neutron star binaries there are two peaks: one for nearly equal-mass systems, and one for systems consisting of a low- and a high-mass neutron star,  $q = 0.6\text{--}0.7$ . The observability-weighted distribution of black hole neutron star binaries is concentrated on systems with mass ratio  $q = 0.3\text{--}0.5$ , while for double black hole binaries the observability-weighted distribution is dominated by massive, nearly equal-mass binaries with  $q > 0.7$ .

**Key words:** gravitational waves – binaries: general.

## 1 INTRODUCTION

We are currently witnessing a large increase in the sensitivity of gravitational wave observatories. LIGO (Abramovici et al. 1992) is already taking data, the development of VIRGO (Bradaschia et al. 1990) shows great advances, and GEO600 (Danzmann et al. 1992) and TAMA300 (Tsubono 1995) are operational. In the coming years an even more sensitive Advanced LIGO will begin taking data. Out of a number of potential sources of gravitational radiation the most promising are probably mergers of compact object binaries, i.e. binaries consisting of black holes (BHs) and/or neutron stars (NSs). These are the only sources for which observations in the electromagnetic domain are consistent with emission of gravitational waves. Present efforts to examine data from gravitational wave detectors show that such detections rely heavily on availability of accurate templates. This provides a case for the importance of accurate merger calculations. The data analysis relies on cross-correlating the data with a number of templates. Scanning a large volume of parameter space requires using a large number of templates and may hinder detection of a real but low-amplitude signal. Any possibility to limit the number of templates required or to show in which region of parameter space a detection is most likely may improve the chances of seeing the gravitational waves.

Thus it is important to ask the following questions: what are the most likely objects to be observed, and what are the most important parameter sets to explore? In order to answer them one

needs to investigate the properties of populations of compact object binaries. Observations provide us with six double neutron star binaries (Thorsett & Chakrabarty 1999; Burgay et al. 2003). The radio-selected sample of double neutron star binaries is biased toward long-lived systems. However, we do not know any black hole neutron star nor double black hole binaries. Therefore inferring the properties of the population of compact object binaries solely on the observations of these few systems may lead to erroneous results. A different approach – binary population synthesis – allows us to investigate the properties of such systems from a theoretical point of view. Binary population synthesis requires, however, a thorough investigation of the systematic uncertainties due to parametrization of various stages of stellar evolution. Population synthesis studies have already been used to estimate the rates and properties of mergers that can be observed by gravitational wave observatories (Lipunov, Postnov & Prokhorov 1997b; Bethe & Brown 1998; Fryer, Burrows & Benz 1998; Portegies Zwart & Yungelson 1998; Belczyński & Bulik 1999; Bulik, Belczyński & Zbijewski 1999; Fryer, Woosley & Hartmann 1999; Belczynski, Kalogera & Bulik 2002c; Nutzman et al. 2004). It has been shown that the observed sample will most likely be dominated by the mergers of double black hole binaries (Lipunov, Postnov & Prokhorov 1997a; Bulik & Belczyński 2003). The distribution of observed chirp masses was found to be a very sensitive indicator of the stellar evolution model while being relatively insensitive to the star-formation rate history and cosmological model (Bulik, Belczyński & Rudak 2004). A preliminary study of the distribution of mass ratios in compact object binaries was presented by Bulik, Belczyński & Kalogera (2003).

\*E-mail: bulik@camk.edu.pl

In this paper we use the STARTRACK population synthesis code to investigate the distribution of masses and mass ratios in the population of compact object binaries. We use a convention where the mass ratio  $q$  in a binary system is defined as the ratio of the lower-mass component to the higher-mass one and therefore is always less than unity. In Section 2 we briefly describe the code, and demonstrate the difference between the volume-limited and flux-limited distributions of masses of compact object binaries. We present the results in Section 3, and conclusions in Section 4.

## 2 CALCULATIONS

We are using the STARTRACK binary evolution code described in detail by Belczynski et al. (2002c). The code is well tested and has been used in various astrophysical applications: analysis of gamma-ray-burst progenitors (Belczynski, Bulik & Rudak 2002b), tracing of evolutionary history of individual binaries (Belczynski & Bulik 2002), and investigation of the mass spectra of compact objects (Belczynski, Bulik & Kluźniak 2002a). The STARTRACK population synthesis code was specifically designed to calculate the merger rates and physical properties of compact object binaries. It was compared with several other codes (e.g. Lipunov et al. 1997b; de Donder & Vanbeveren 1998; Portegies Zwart & Yungelson 1998; Fryer et al. 1999; Nelemans et al. 2001). The comparisons showed some differences; however, they were understood within the different model assumptions. Since STARTRACK was designed to deal mostly with systems containing NSs and BHs, our input physics was updated and revised as compared to the other codes with respect to compact object formation. As a result we have recognized new evolutionary NS–NS formation scenarios, and we have shown that massive stellar BH may dominate the population of double compact objects ( $\sim 10 M_{\odot}$ ) observed in gravitational waves. Last, but not least, our predictions of NS–NS Galactic coalescence rates (Belczynski et al. 2002c) are in good agreement with the most recent constraints obtained from the observed sample of these systems (Kalogera et al. 2001; Kim, Kalogera & Lorimer 2003).

### 2.1 Standard model

Within the code the evolution of single stars is parametrized by the modified formulae of Hurley, Pols & Tout (2000). The single-star evolution includes such stages as the main sequence, evolution on the Hertzsprung gap, red giant branch, core helium burning, asymptotic giant branch, and evolution of helium stars. Two major modifications include low-mass helium-star evolution and calculation of compact object masses. In particular, following a number of studies (Delgado & Thomas 1981; Habetts 1987; Avila-Reese 1993; Woosley, Langer & Weaver 1995) we allow the low-mass helium stars ( $\leq 4 M_{\odot}$ ) to develop deep convective envelopes. The presence of a convective envelope plays an important role in the behaviour of the donor star in the Roche lobe overflow event, and may eventually lead to the development of dynamical instability and common-envelope (CE) evolution, and possible tightening of the binary orbit.

The original Hurley et al. (2000) formulae are used to calculate the final CO core mass of a given compact object progenitor at the time of a supernova/core-collapse event. We use the stellar models of Woosley (1986) to obtain the mass of the final FeNi core corresponding to a given CO core mass. The FeNi core is collapsed to form a protoneutron star, and then we use the results of the core-collapse hydrodynamical calculation of Fryer (1999) to calculate the amount of fall-back material and the final mass of the newly

formed compact object. We use the following algorithm to derive the masses of a newly formed compact object  $M_{\text{rem}}$ :

$$M_{\text{rem}} = \begin{cases} M_{\text{FeNi}} & M_{\text{CO}} \leq 5 M_{\odot} \\ M_{\text{FeNi}} + f_{\text{fb}}(M - M_{\text{FeNi}}) & 5 < M_{\text{CO}} < 7.6 \\ M & M_{\text{CO}} \geq 7.6 M_{\odot} \end{cases} \quad (1)$$

where  $M_{\text{FeNi}}$  is the mass of the FeNi core,  $M_{\text{CO}}$  is the mass of the CO core,  $M$  is the total mass of the star prior to the explosion, and  $f_{\text{fb}}$  is the fall-back factor,  $0 < f_{\text{fb}} < 1$  depending on the mass of the star. This simple formula represents well the results of detailed numerical calculations. We do verify the sensitivity of our results to changes in the particular numerical values in equation (1), see, e.g. model O below. Varying stellar evolution parameters like the strength of winds, or metallicity leads to different core masses for a star of given initial mass and also alters the initial final mass relation for single stars. We find that NSs are formed without a significant amount of fall-back material, while BHs are formed either directly (prompt collapse of a massive star) or through partial fall-back of material on to the protoneutron star.

The binary evolution takes into account orbit changes due to wind mass loss, and tidal interactions. Wind mass-loss rates are adopted from Hurley et al. (2000) and they depend on the stellar parameters of the mass-losing component (its composition, mass and evolutionary stage). Specific mass-loss rates are adopted for naked helium stars, luminous blue variables and pulsating stars. In stable mass transfer (MT) calculations we allow for non-conservative evolution. We assume that part ( $f_a$ ) of the transferred material is accreted on to the companion star, while the rest is ejected from the system with specific angular momentum ( $j$ , expressed in units of the binary angular momentum). In our standard model we adopt  $f_a = 0.5$  and  $j = 1$ . If the Roche lobe overflow (RLOF) episode is dynamically unstable, we follow the inspiral through the common-envelope phase. If the system avoids the merger, we calculate the final orbital separation using the standard energy conservation based prescription of Web-bink (1984). The evolution through the CE phase depends crucially on the efficiency of the orbital energy input into the donor envelope ( $\alpha_{\text{CE}}$ ) and the specific binding energy of the envelope ( $\lambda$ ). Only the product of these two largely uncertain quantities enters the calculation, and we use  $\alpha_{\text{CE}} \times \lambda = 1$  in the standard model; however we also check the sensitivity of the results to this parameter. During the CE inspiral we allow for hypercritical accretion on to NSs and BHs (e.g. Blondin 1986; Chevalier 1989, 1993; Brown 1995). As a result several tenths of a solar mass may be accreted on to the compact object, and in particular the top-heavy NSs may collapse and form BHs. The full description of the hypercritical accretion treatment is given in the appendix of Belczynski et al. (2002c).

Supernovae (SN) explosions are treated in detail. The explosion takes place at a randomly selected place on the orbit. We allow for explosions on eccentric orbits, for uncircularized systems. We take into account the instantaneous mass and angular momentum loss from the binary system. Also a natal kick is added to the orbital velocity of the newly born compact object to account for the SN asymmetry. Kicks are selected from the bimodal distributions of Cordes & Chernoff (1998), a weighted sum of two Maxwellians, one with  $\sigma = 175 \text{ km s}^{-1}$  (80 per cent) and the second with  $\sigma = 700 \text{ km s}^{-1}$  (20 per cent). A binary is either disrupted in the explosions, in which case we stop the evolution, or if it survives we follow the evolution on the new binary orbit.

The initial mass of the primary  $M_{\text{zams}}^1$  is drawn from a power law initial mass function (IMF) distribution  $\propto M^{-2.7}$  (Scalo 1986) within the range  $8\text{--}100 M_{\odot}$ . The secondary mass is obtained as

**Table 1.** Population synthesis models. We list the number of coalescing compact object binaries produced in each simulation. For detailed model descriptions see Sections 2.1 and 2.2.

Model	Description	$N$ produced
A	standard model described in Section 2.1	5761
B1	zero kicks	21535
B7	single Maxwellian with $\sigma = 50 \text{ km s}^{-1}$	17747
B11	single Maxwellian with $\sigma = 500, \text{ km s}^{-1}$	2155
B13	Paczynski (1990) kicks with $V_k = 600 \text{ km s}^{-1}$	8270
C	no hypercritical accretion on to NS/BH in CEs	4798
E1	CE efficiency: $\alpha_{\text{CE}} \times \lambda = 0.1$	894
E2	CE efficiency: $\alpha_{\text{CE}} \times \lambda = 0.5$	3489
E3	CE efficiency: $\alpha_{\text{CE}} \times \lambda = 2$	8504
F1	mass fraction accreted in non-cons. MT: $f_a = 0.1$	2483
F2	mass fraction accreted in non-cons. MT: $f_a = 1$	4644
G1	wind decreased by $f_{\text{wind}} = 0.5$	9395
G2	wind changed by $f_{\text{wind}} = 2$	5517
J	primary mass: $\propto M_1^{-2.35}$	8220
L1	angular momentum of material lost in non-cons. MT: $j = 0.5$	6660
L2	angular momentum of material lost in non-cons. MT: $j = 2.0$	5547
M1	initial mass ratio distribution: $\Phi(q) \propto q^{-2.7}$	852
M2	initial mass ratio distribution: $\Phi(q) \propto q^3$	11225
O	partial fall-back for $5.0 < M_{\text{CO}} < 14.0 M_{\odot}$	4116
S	all systems formed in circular orbits	4667
Z1	metallicity: $Z = 0.01$	5199
Z2	metallicity: $Z = 0.0001$	7074

$M_{\text{zams}}^2 = qM_{\text{zams}}^1$ , where  $q$  is the mass ratio and is drawn from a flat distribution (Kuiper 1935). We allow for eccentric initial orbits, and the eccentricities are drawn from a thermal distribution  $\propto e$  (Heggie 1975; Duquennoy & Mayor 1991). Finally, the orbital separation distribution is taken to be flat in  $\log a$  (Abt 1983), and separations are chosen from a few (so the stars are not formed at the contact configuration) up to a maximum of  $10^5$  solar radii. We evolve our stars for a maximum  $T_{\text{Hubble}} = 15 \text{ Gyr}$ . The evolutionary model described above is chosen as our reference (standard) model and marked with the letter ‘A’ in the following figures and tables.

## 2.2 Parameter study

In order to assess the robustness of the results we investigate 20 extra different models of stellar evolution, where we vary the parameters describing various stages of stellar and binary evolution. The models used are listed in Table 1. The range of models represents the current state of knowledge and uncertainties about binary evolution. All models are calculated with  $2 \times 10^6$  initial binaries each.

In models marked with the letter ‘B’ we vary the distribution of natal kicks compact objects receive when they are formed. This is a rather uncertain part of the evolutionary model as we still do not know the mechanism behind the SN/core-collapse asymmetry (Buras et al. 2003). Therefore, we change the kicks quite drastically, from a rather unrealistic model with no kicks (B1) to the very strong kicks of model B11. The higher the kicks, the fewer compact object binaries we form, since the higher kicks tend to disrupt the progenitor systems. This is one of the most important parameters as far as the number of compact object binaries is concerned (close to an order of magnitude change).

Since the CE evolution is another highly uncertain part of our evolutionary scheme, in models ‘E’ we change the efficiency with which orbital energy is transformed into unbinding the envelope of the donor star, while in model ‘C’ we turn off the accretion on

to compact objects during that very short-lived phase. In models with small CE efficiency (E1–E2) it is found that the number of compact object binaries is significantly reduced. This is due to the fact that many binaries, evolving through the CE phase, will merge, thus aborting compact object binary formation. On the other hand, increase of the efficiency (E3) or shutting down the accretion at the CE phase does not play a very important role on the number of formed compact object binaries.

In models ‘F’ and ‘L’ we consider the results for different treatments of the stable MT phases. In particular, in model F2 we consider the case of conservative evolution (all mass and angular momentum transferred to the companion). Change of the MT mode from non-conservative (standard model) to conservative evolution (F2) does not change the numbers by much. Model F1 with highly non-conservative evolution decreases the numbers of formed compact object binaries rather significantly, but it is rather improbable, since the estimated material loss is probably not as high as assumed in model F1 (Meurs & van den Heuvel 1989). Since we have adopted quite a large value for the specific angular momentum of lost material in non-conservative MT episodes, we should really consider only model L1 with lowered specific momentum leaving the binary. As we see from Table 1, the numbers in model L1 are almost the same as for the standard model. We thus conclude that the treatment of non-conservative MT phases does not have a great influence on the number of compact object binaries.

Winds of massive stars may play an important role in the population of compact objects. In model G1 we decrease all the wind mass-loss rates by a factor of 2. The weaker the winds, the more massive compact objects are formed, and more BHs are formed as compared to NSs. However, the total number of compact object binaries is basically unchanged in this model.

The flatter IMF slope of model J slightly increases (as the slope was not changed by much) the number of heavy stars (progenitors of compact objects) and thus leads to a slight increase in the number of compact object binaries. The IMF slope for massive stars is rather

well determined (Kroupa & Weidner 2003), and as expected the small change does not affect the population.

The change of initial mass ratio distribution may have a severe effect on the numbers of compact object binaries (models M1–M2). In model M1 most of the progenitor systems are formed with extremely small mass ratios. Therefore, once they reach the first MT phase, it is usually dynamically unstable, leading to inspiral and merger of components, aborting the formation of a compact object binary. This explains the small number of formed binaries in model M1, and warrants survival of systems (large numbers of compact object binaries) with rather equal masses in model M2. Since the initial mass-ratio distribution is not easily measurable and constrained, models M1–M2, although rather extreme, should be taken into account in further analysis.

Finally, several other models do not have much influence on the production efficiency of compact object binaries. These include models with different metallicities (Z1–Z2), different assumptions on initial eccentricities (S) and finally the model in which we change the fall-back regime in the formation of compact object binaries (O).

The masses of compact objects are strongly affected in some of the models. In particular the masses change quite drastically in models G1 and G2 where the stellar winds are changed. Decreasing the stellar winds (model G1) allows the stars to develop more massive cores and consequently leads to higher masses of the compact objects formed. A similar effect is connected with decreasing the metallicity (models Z1 and Z2), since lower-metallicity stars have weaker winds. On the other hand, within model G2, where the winds are artificially increased, massive stars do not have the time to develop massive cores and no compact objects above  $3 M_{\odot}$  are produced. The masses of the compact objects are also affected by varying the parameters in equation (1). In model O we increase the upper bound of the fall-back range to  $14 M_{\odot}$ . This leads to smaller masses of the black holes produced as even for high-mass cores some fraction of the mass is still expelled. The population of compact object binaries in model E1, with reduced common-envelope efficiency, contains additional systems with massive black holes. Within model C we turn off the hypercritical accretion on to compact objects in common-envelope events. This primarily influences the masses of neutron stars and low-mass black holes as they have no possibility to increase significantly.

### 2.3 Distributions of masses and mass ratios

In the output we note the masses of the compact objects in each binary and the lifetimes: the stellar lifetime from the formation at the zero age main sequence to formation of a double compact object, and the lifetime as a double compact object binary until it merges due to gravitational wave emission. We denote the sum of the two lifetimes as the total lifetime,  $T$ , of the binary.

In this calculation we assume for simplicity that the space is Euclidean. We denote the masses of the components in each binary as  $m_1^i$  and  $m_2^i$ , and the mass ratio is  $q = m_1^i/m_2^i < 1$ . The formation rate of compact object binaries with a given mass ratio  $q$ , the mass of the primary  $m_2$  (the greater of the two masses), and the lifetime  $T$  at a given cosmic time  $t$  is

$$\frac{d^3 F(m_2, q, T, t)}{dm_2 dq dT} = \frac{S(t) f_{\text{sim}}}{\langle M_* \rangle N_{\text{tot}}} \times \sum_{i=1}^{N_{\text{CCOB}}} \delta(m_2 - m_2^i) \delta(q - q^i) \delta(T - T^i), \quad (2)$$

where  $S(t)$  is the star-formation rate at time  $t$ ,  $f_{\text{sim}}$  is the fraction of stars out of the total population that we simulate,  $\langle M_* \rangle$  is the average

mass of a binary in the stellar population, and  $N_{\text{CCOB}}$  is the number of coalescing compact object binaries formed in a simulation of  $N_{\text{tot}}$  binaries. Our aim is to calculate the observed merger rate by an observer on Earth at present, which we denote as  $t_0$ . The coalescence rate at a distance  $r$  from the observer is then given by

$$\frac{d^2 f_{\text{coal}}(r)}{dm_2 dq} = \int dt' \frac{dF(m_2, q, t', t_0 - r/c - t')}{dm_2 dq dT}. \quad (3)$$

Inserting equation (3) into (2) we obtain

$$\frac{d^2 f_{\text{coal}}(r)}{dm_2 dq} = \frac{f_{\text{sim}}}{\langle M_* \rangle} N_{\text{tot}}^{-1} \times \sum_{i=1}^{N_{\text{CCOB}}} \delta(m_2 - m_2^i) \delta(q - q^i) S(t_0 - r/c - T^i). \quad (4)$$

The observed rate is obtained by integrating equation (4) over the volume in which the binaries are observable:

$$\frac{d^2 R}{dm_2 dq} = \int_{V(m_2, q)} dV \frac{df_{\text{coal}}(r)}{dm_2 dq}. \quad (5)$$

We note that for a constant star-formation rate the lifetimes of the binaries do not enter the observed rate.

We first calculate a volume-limited distribution of masses, i.e. we assume that all binaries coalescing in a given volume  $V$  are observable regardless of the mass  $m_2$  and the mass ratio  $q$ . This corresponds to observing, for example, the entire population of a given galaxy or a galaxy cluster. Here we also assume that the star-formation history was constant. The normalized volume-limited distribution of masses and mass ratios is

$$P(q, m_2) = N_{\text{CCOB}}^{-1} \sum_{i=1}^{N_{\text{CCOB}}} \delta(q - q^i) \delta(m_2 - m_2^i). \quad (6)$$

In the case of realistic detectors the volume of integration in equation (5) will depend on  $m_2$  and  $q$ . Our calculation of the distribution of masses and mass ratios relevant for detecting merging binaries with gravitational waves follows the calculations presented earlier in Bulik & Belczyński (2003). Here again we assume that the star-formation rate was flat and that the Universe is Euclidean and uniformly filled with stars. The signal-to-noise ratio (S/N) in high-frequency gravitational wave detectors from an inspiral of a stellar mass binary is given by (Finn & Chernoff 1993; Bonazzola & Marck 1994; Flanagan & Hughes 1998)

$$(S/N) = \frac{A_i}{d} \left( \frac{\mathcal{M}}{M_{\odot}} \right)^{5/6}, \quad (7)$$

where  $\mathcal{M} = (m_1 m_2)^{0.6} (m_1 + m_2)^{-0.2}$  is the chirp mass,  $d$  is the distance, and the  $A_i$  depend on the details of a particular detector. Thus coalescence of a binary with a chirp mass  $\mathcal{M}^i$  will be visible up to a distance proportional to  $(\mathcal{M}^i)^{5/6}$  and the volume of integration in equation (5) will be  $V^i \propto (\mathcal{M}^i)^{5/2}$ . The observability-weighted distribution of masses and mass ratios is therefore

$$P_{\text{obs}}(q, m_2) = K^{-1} \sum_i V_i \delta(q - q^i) \delta(m_2 - m_2^i), \quad (8)$$

where  $K = \sum_i V_i$ . Again the lifetimes of the binaries do not enter the weights in equation (8) because of the assumption of constant star-formation rate history. This distribution is more realistic as it corresponds to the case of an instrument with sensitivity allowing it to detect binary coalescences in a large ensemble of galaxies. Relaxation of the assumption of constant star formation and taking into account a realistic cosmological model has been discussed by Bulik et al. (2004) for the case of the distribution of observed chirp masses and was shown not to be significant.

### 3 RESULTS

In the following we will assume that the maximum mass of a neutron star is  $3 M_{\odot}$ . All objects above this value will be considered as black holes. In our simulations the minimum mass of a neutron star is  $1.2 M_{\odot}$ . Thus we can classify all binaries as double neutron star (NSNS), black hole neutron star (BHNS), or double black hole binaries (BHBH). These three categories will be analysed separately. We will present the distributions of binary parameters in the space spanned by the mass of the primary (the more massive component of a compact object binary) and the mass ratio  $q$ .

#### 3.1 NSNS binaries

We present the volume-limited distributions of  $q$  and  $m_2$  obtained in the framework of model A in the top panels of Fig. 1. The volume-limited distribution for the case of NSNS systems (top-left panel) exhibits a peak for systems with nearly equal masses just above the minimal mass of a neutron star. This roughly corresponds to the observations of pulsars where most systems have similar masses. There is, however, a long tail in the distribution extending to systems with large mass of the primary, and low mass ratio. These are systems

consisting of a neutron star with a mass near the maximum value and a companion neutron star with a low mass. Such systems have a chirp mass about 1.5 times larger than the binaries from the above mentioned peak. Therefore in the flux-limited distribution – top-right panel in Fig. 1 – these low mass-ratio systems are showing up more prominently. It is, however, possible that the maximum mass of a neutron star is lower than  $3 M_{\odot}$  and some of the systems shown here harbour low-mass black holes rather than neutron stars. However, even for the maximum mass of a neutron star of  $2.0 M_{\odot}$  there is still a large fraction of low- $q$  systems in the flux-limited distribution. We have examined all 21 models listed in Table 1 and nearly all the models show a similar pattern in both the volume-limited and flux-limited distributions. There is one exception – model C – for which we present the relevant distributions in the bottom panels of Fig. 1. In this model we turn off the possibility of hypercritical accretion on to a compact object in the common-envelope phase. This effectively shuts off the possibility of increasing significantly the mass of a neutron star through accretion. Therefore in the volume-limited distribution there is quite a large concentration of systems with both masses below  $1.5\text{--}1.6 M_{\odot}$ , and small number of binaries with low mass ratios. Consequently in the flux-limited distribution the binaries with low mass ratio are nearly absent in contrast to

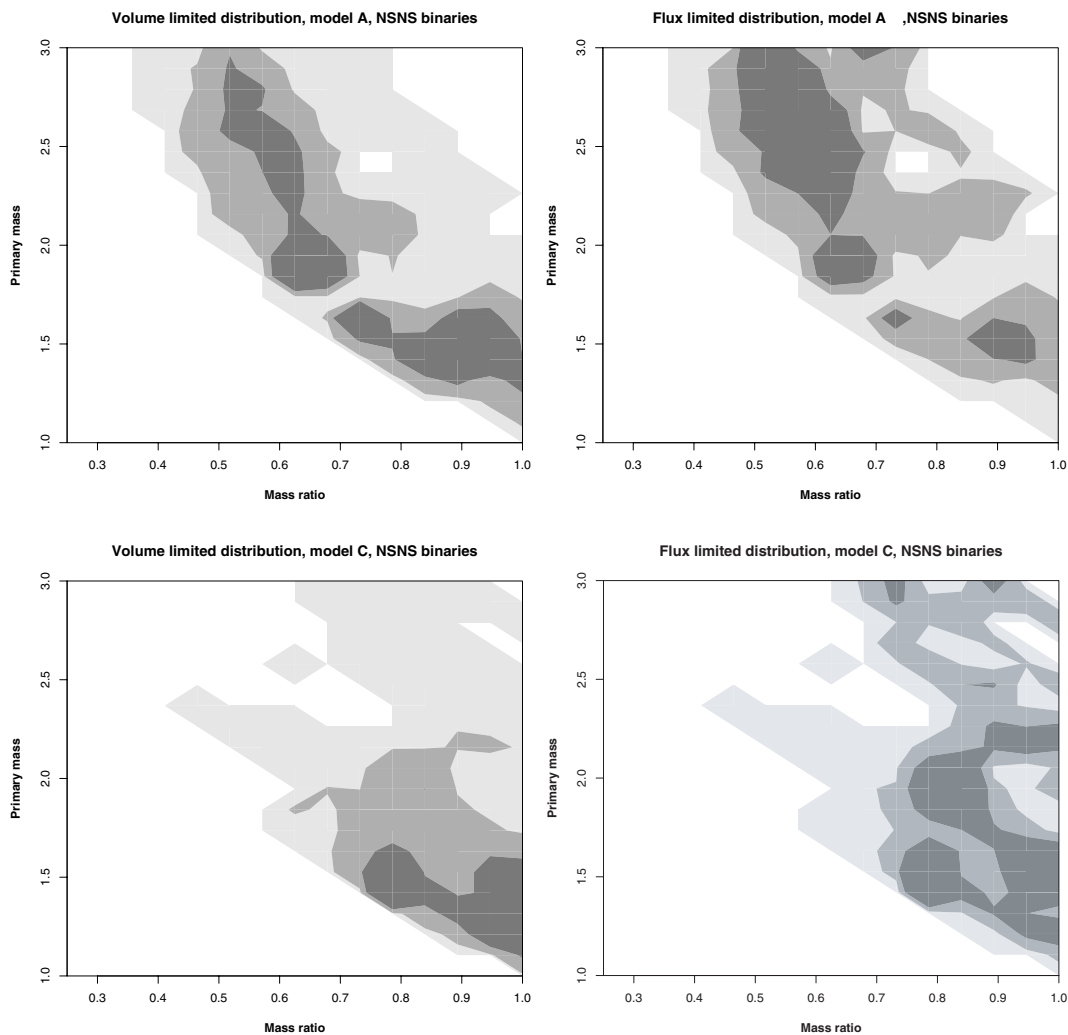


**Figure 1.** The volume-limited and observability-weighted distributions of parameters of compact NSNS binaries obtained within model A – top panel – and model C – bottom panel. The region in dark grey encompasses 68 per cent of the systems, the medium grey corresponds to 95 per cent, and the light grey corresponds to all binaries in the simulation.

model A. However, the 68 per cent contour includes systems with  $q > 0.75$  and  $m_2 \approx 2.0 M_\odot$ , as well as some binaries with  $q \approx 0.75$  and the mass of the primary close to the maximal mass of a neutron star in our model.

### 3.2 BHNS binaries

We present the volume-limited and the flux-limited distributions of  $q$  and  $m_2$  in Fig. 2. The top panel of Fig. 2 corresponds to the standard

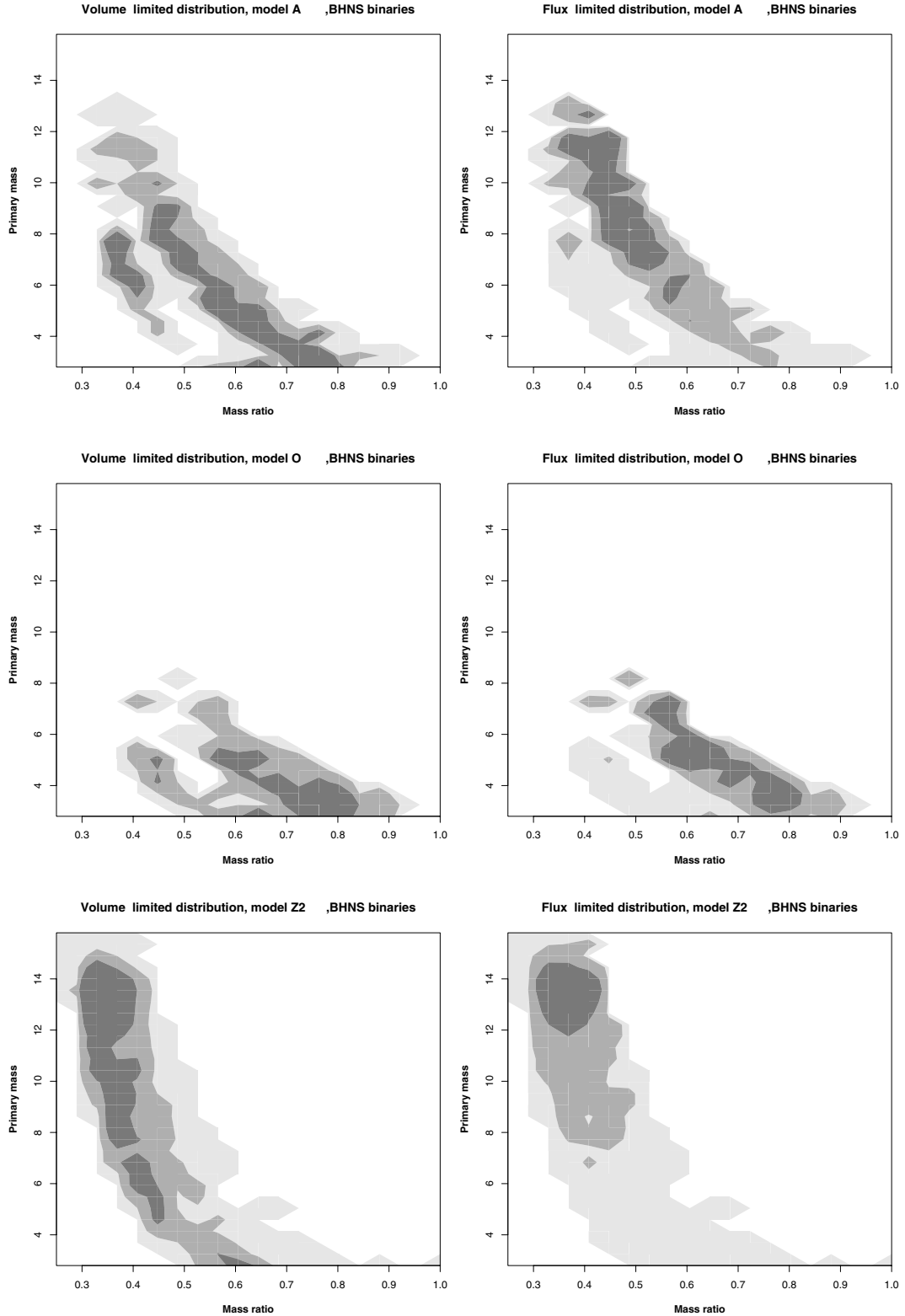


**Figure 2.** The volume-limited and observability-weighted distributions of the parameters of BHNS binaries within model A (top panel), model O (middle panel) and model Z2 (bottom panel). The region in dark grey encompasses 68 per cent of the systems, the medium grey corresponds to 95 per cent, and the light grey corresponds to all binaries in the simulation.

model A. The volume-limited distribution shows a large number of binaries along a stripe stretching from  $q \approx 0.7$  and  $m_2 \approx 4 M_\odot$  to  $q \approx 0.2$  and  $m_2 \approx 10 M_\odot$ . Systems above and to the right of this stripe would be classified as BHBH binaries. The volume-limited distribution is dominated by binaries with low-mass black holes. In the flux-limited distribution the binaries with higher-mass black holes and low mass ratios start to play an important role. This is due to the balance between the falling mass function and the increase in the chirp mass with increase of the mass of the primary. For nearly all models this leads to dominance of binaries where the black hole primary has a mass between 6 and 12  $M_\odot$ , and the mass ratio is somewhere from 0.3 for the most massive black holes to 0.5 for the moderate-mass ones.

After examining the 21 models of Table 1 in the case of BHNS binaries one can distinguish two other classes of models with different distributions of binary parameters. The first class consists of models L2, M2 and O. For this models we show a representative case (model O) in the middle panel of Fig. 2. The common characteristic of this class of models is that the population of black holes in binaries lacks the very massive ones for various reasons. In the case of model O shown in Fig. 2 this is because we increase the range of masses of fall-back formation of black holes. Within the models E1, L2, M2 such binaries have a smaller chance of formation because of altering the treatment of the mass transfer events. In consequence there are very few low mass-ratio BHNS binaries and the volume-limited distribution is very similar to the flux-limited one.

A separate class consists of models E1, Z2 and G1. In their case high-mass black holes are easily formed, because of a decrease of strength of stellar winds (Z2 and G1). Model E1 favours survival of systems with high-mass first-born stars and leads to effective production of extreme mass ratio compact object binaries. We present the two distributions for the case of model Z2 in the bottom panel of Fig. 2. Here the volume-limited distribution is dominated by a nearly vertical stripe at  $q \approx 0.2$ . In the flux-limited distribution the binaries with high-mass primaries  $m_2 \approx 12 M_\odot$  and  $0.1 < q < 0.3$  are dominant simply because of their high chirp mass.

### 3.3 BHBH binaries

The case of BHBH binaries is presented in Fig. 3. The top panel corresponds to model A. The volume-limited distribution fills more or less uniformly the region allowed for the BHBH binaries. In the flux-limited distribution there is a preference for the high mass ratio (nearly equal mass) and high mass systems, i.e. those filling the top-right corner of the plot. Thus the flux-limited distribution is dominated by the systems with  $q < 0.6$  and  $m_2$  near the maximum mass produced in a given model. All models seem to follow this general trend.

In models O the maximum mass of a black hole is decreased. We present the results of a calculation using model O, in the middle panel of Fig. 3. In this case the volume-limited distribution also fills nearly uniformly the region allowed for black holes. However because of its smaller size the range of chirp masses for a given mass ratio is not as large and the flux-limited distribution is only slightly shifted to higher masses with respect to the volume-limited one.

Another special case – model E1 – is presented in the bottom panel of Fig. 3. Here because of the lowered CE efficiency, formation of equal-mass compact object binaries is favoured, while extreme-mass binaries are preferentially formed. The volume-limited distribution in this case is dominated by systems with mass ratio in the range  $0.4 < q < 0.6$  and a tail extending to  $q = 0.8$ .

Models of the class that favours production of massive black holes (Z2, G1) do not lead to qualitatively different results from model A. In these models the flux-limited distributions tend to concentrate around binaries with higher mass ratio,  $q > 0.7$ , and higher total masses than in the standard model A.

## 4 CONCLUSIONS

We have calculated the expected distributions of masses and mass ratios of compact object binaries to be observed in gravitational waves. The results are based on the STARTRACK binary population synthesis code. For most of the models the observability-weighted distribution of double neutron star systems has two peaks: one with the mass ratio almost unity and both masses near the smallest mass allowed for neutron stars, and another with small mass ratio, consisting of stars with mass near the maximum mass of a neutron star in a binary with a star close to the minimum mass. The reality of this second peak depends on the assumed maximum mass of a neutron star: the lower the maximum mass of a neutron star the smaller the small mass ratio peak. The distribution of black hole neutron star binaries peaks at mass ratios between 0.3 and 0.5. The bulk of observed double black hole binaries has mass ratios above 0.7. We have shown that these results are rather generic and depend weakly on the choice of a particular model of stellar evolution.

The crucial parameter determining the shape of the distribution of the observed NSNS binaries is inclusion of the hypercritical accretion on to compact objects in common-envelope events. In the case of BHNS and BHBH binaries the most important parameters are those that alter the masses of the black holes in such binaries, and the common-envelope efficiency. The masses may be altered either due to the mechanism of compact object formation in supernova explosions, or due to the particular treatment of mass transfer events. The distribution of the BHNS binary parameters is most sensitive to these changes. However, we must note that the observed sample is dominated by the BHBH binaries. For most models more than 90 per cent of observed systems are double black hole binaries (Bulik & Belczyński 2003).

These results can be used as a guideline for choosing the initial conditions in numerical simulations of mergers of compact object binaries. Additionally the results of this work can be used in preparing data analysis software using templates for detection of gravitational waves from compact object inspiral. Coalescences of BHBH binaries dominate the observed sample, and we find that the observability-weighted distribution is peaked around nearly equal-mass binaries. We find that in most models the flux-limited sample of NSNS binaries contains a large fraction of unequal-mass objects. We conclude that the initial search for gravitational waves from coalescences of compact object binaries should concentrate on BHBH coalescences with mass ratio close to unity, and the low mass ratio NSNS coalescences should be taken into account.

Finally, we note that this work only includes binaries that evolved in galaxies, and neglects all possible effects, like multiple stellar interactions that are relevant for evolution in dense stellar clusters.

## ACKNOWLEDGMENTS

This work was supported by the KBN grant 5P03D01120 and Technology Programme EPAN-M.43/2013555 and the EU Programme ‘Improving the Human Research Potential and the Socio-Economic Knowledge Base’ (Research Training Network Contract HPRN-CT-2000-00137). KB is a Lindheimer Fellow. We are grateful to the referee for comments on this manuscript.

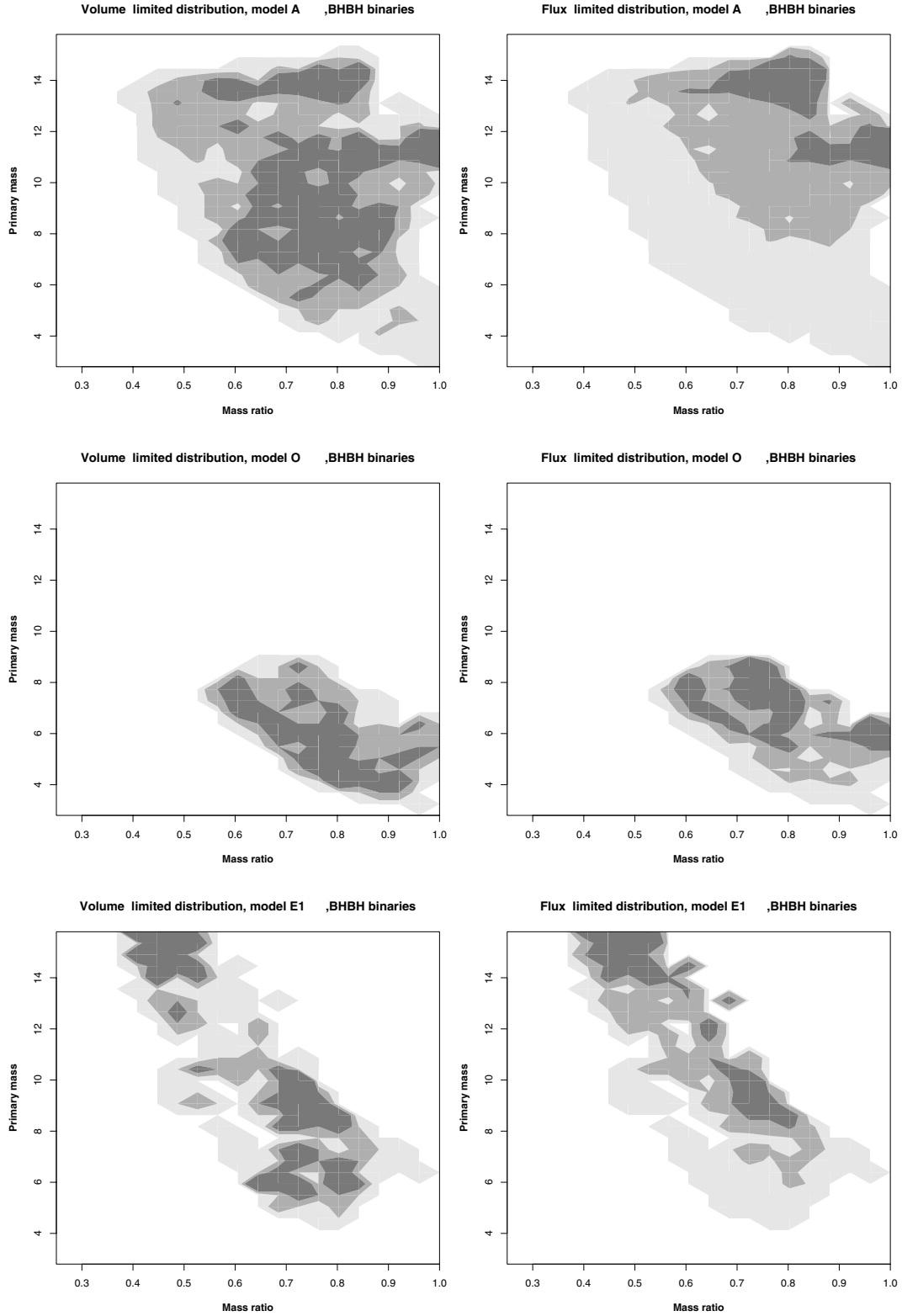


**Figure 3.** The volume-limited and observability-weighted distributions of the parameters of BHBH binaries within model A (top panel), and model O (bottom panel). The region in dark grey encompasses 68 per cent of the systems, the medium grey corresponds to 95 per cent, and the light grey corresponds to all binaries in the simulation.

**REFERENCES**

Abramovici A., Althouse W. E., Drever R. W. P. et al., 1992, *Sci*, 256, 325  
 Abt H. A., 1983, *ARA&A*, 21, 343

Avila-Reese V., 1993, *Rev. Mex. Astron. Astrof.*, 25, 79  
 Belczyński K., Bulik T. 1999, *A&A*, 346, 91  
 Belczynski K., Bulik T., 2002, *ApJ*, 574, L147  
 Belczynski K., Bulik T., Kluzniak W. L., 2002a, *ApJ*, 567, L63

- Belczynski K., Bulik T., Rudak B., 2002b, *ApJ*, 571, 394  
 Belczynski K., Kalogera V., Bulik T., 2002c, *ApJ*, 572, 407  
 Bethe H. A., Brown G. E., 1998, *ApJ*, 506, 780  
 Blondin J. M., 1986, *ApJ*, 308, 755  
 Bonazzola S., Marck J. A., 1994, *Ann. Rev. Nucl. Part. Sci.*, 45, 655  
 Bradaschia et al., 1990, *Nucl. Instr. Methods Phys. Res.*, A, 289, 518  
 Brown G. E., 1995, *ApJ*, 440, 270  
 Bulik T., Belczyński K., 2003, *ApJ*, 589, L37  
 Bulik T., Belczyński K., Zbijewski W., 1999, *MNRAS*, 309, 629  
 Bulik T., Belczyński K., Kalogera V., 2003, in Cruise M., Saulson P., eds, *Proc. SPIE, Gravitational-Wave Detection*. Int. Soc. Opt. Eng., Bellingham, WA, p. 146  
 Bulik T., Belczyński K., Rudak B., 2004, *A&A*, 415, 407  
 Buras R., Rampp M., Janka H.-T., Kifonidis K., 2003, *Phys. Rev. Lett.*, 90, 241101  
 Burgay M. et al., 2003, *Nat*, 426, 531  
 Chevalier R. A., 1989, *ApJ*, 346, 847  
 Chevalier R. A., 1993, *ApJ*, 411, L33  
 Cordes J. M., Chernoff D. F., 1998, *ApJ*, 505, 315  
 Danzmann K. et al., 1992, in *Lecture Notes in Physics*, 410, 184  
 de Donder E., Vanbeveren D., 1998, *A&A*, 333, 557  
 Delgado A. J., Thomas H.-C., 1981, *A&A*, 96, 142  
 Duquennoy A., Mayor M., 1991, *A&A*, 248, 485  
 Finn L. S., Chernoff D. F., 1993, *Phys. Rev. D*, 47, 2198  
 Flanagan É. É., Hughes S. A., 1998, *Phys. Rev. D*, 57, 4535  
 Fryer C., Burrows A., Benz W., 1998, *ApJ*, 496, 333  
 Fryer C. L., Woosley S. E., Hartmann D. H., 1999, *ApJ*, 526, 152  
 Habetz G. M. H. J., 1987, *A&AS*, 69, 183  
 Heggie D. C., 1975, *MNRAS*, 173, 729  
 Hurley J. R., Pols O. R., Tout C. A., 2000, *MNRAS*, 315, 543  
 Kalogera V., Narayan R., Spergel D. N., Taylor J. H., 2001, *ApJ*, 556, 340  
 Kim C., Kalogera V., Lorimer D. R., 2003, *ApJ*, 584, 985  
 Kroupa P., Weidner C., 2003, *ApJ*, 598, 1076  
 Kuiper G. P., 1935, *PASP*, 47, 15  
 Lipunov V. M., Postnov K. A., Prokhorov M. E., 1997a, *New Astron.*, 2, 43  
 Lipunov V. M., Postnov K. A., Prokhorov M. E., 1997b, *MNRAS*, 288, 245  
 Meurs E. J. A., van den Heuvel E. P. J., 1989, *A&A*, 226, 88  
 Nelemans G., Yungelson L. R., Portegies Zwart S. F., Verbunt F., 2001, *A&A*, 365, 491  
 Nutzman P., Kalogera V., Finn L. S., Hendrickson C., Belczynski K., 2004, *ApJ*, submitted (astro-ph/0402091)  
 Paczynski B., 1990, *ApJ*, 348, 485  
 Portegies Zwart S. F., Yungelson L. R., 1998, *A&A*, 332, 173  
 Scalo J. M., 1986, *Fundam. Cosmic Phys.*, 11, 1  
 Thorsett S. E., Chakrabarty D., 1999, *ApJ*, 512, 288  
 Tsubono K., 1995, in Coccia E., Pizzella G., Ronga F., eds, *First Edoardo Amaldi Conf., Gravitational Wave Experiments*. World Scientific, Singapore, p. 112  
 Webbink R. F., 1984, *ApJ*, 277, 355  
 Woosley S. E., 1986, in Hauck B., Maeder A., Meynet G., eds, *Saas-Fee Advanced Course 16: Nucleosynthesis and Chemical Evolution*. Geneva Obs., Sauverny, 1  
 Woosley S. E., Langer N., Weaver T. A., 1995, *ApJ*, 448, 315

This paper has been typeset from a  $\text{\TeX}/\text{\LaTeX}$  file prepared by the author.